Proceedings of the ASME 27th International Conference on Offshore Mechanics and Arctic Engineering
OMAE2008
June 15-20, 2008, Estoril, Portugal

OMAE2008-57765

AN EXPERIMENTAL INVESTIGATION OF ROLL MOTIONS OF AN FPSO

Paulo T. T. Esperança, Joel S. Sales Jr.
Department of Naval and Ocean Engineering,
Federal University of Rio de Janeiro
ptarso@peno.coppe.ufrj.br
joel@peno.coppe.ufrj.br

Stergios Liapis, João Paulo J. Matsuura
Shell International Exploration and Production,
Bellaire Technology Center
Stergios.Liapis@shell.com
Joao.Matsuura@shell.com

Wes Schott
Wes Schott International
Wes.Schott@wes-schott-international.com

ABSTRACT

FPSO roll motions can be major contributor to riser fatigue. This is especially true in regions where wind, waves and currents are non-collinear. Roll motions as high as 23 degrees have been reported in the Campos Basin. The most common roll mitigation strategy consists of adding bilge keels to the FPSO. Motivation for this work came from a need to develop a better understanding of roll motions as a function of bilge keel width. In addition to roll motions, the hydrodynamic forces on the bilge keels were measured.

A series of tests were conducted at the LabOceano offshore basin. This new facility has a length of 4 0 m, a width of 30 m, a depth of 15 m and is equipped with a multi-flap wave generator on one side. A ship-shaped FPSO design with sponsons for a deepwater offshore development in Brazil was tested. It has a length of 316 m, a breadth of 57.2 m and a draft of 28.3 m. A 1:70 scale model was constructed. A horizontal soft mooring system consisting of four lines with springs was used.

Regular waves of different amplitudes as well as random waves were generated in the basin. Two different loading conditions, ballast (draft = 6.7 m) and loaded (draft = 21.7 m), as well as three wave headings, beam seas (90º), and quartering seas (22.5º, 45º) were considered. Tests were undertaken for four bilge keel configurations, corresponding to a case without bilge keels, as well as bilge keels of 3 different widths (1 m, 2 m and 3 m). In all cases, the bilge keels had a length of 200 m.

An optical system was used to measure ship motions in all six degrees of freedom. The hydrodynamic loads on the bilge keels were measured using strain gages.

INTRODUCTION

The purpose of the model tests was to measure the roll motions of an FPSO in waves and the associated bilge keel forces. Knowledge of the magnitude of the roll motions (related to the roll damping) help define the need and size of the bilge keels, while knowledge of bilge keel forces is primarily of interest for structural design, especially for wide bilge keels.

Bilge keels with three different widths were instrumented with strain gauges. Two loading conditions were tested: fully loaded and ballast. The model responses were taken for regular and irregular waves, for three wave incidences. Two bimodal seas were tested for each loading condition.

NOMENCLATURE

ε_x	Strain in the x direction;
ε_y	Strain in the y direction;
ν	Poisson's ratio;
E	Modulus of elasticity of the material;
D	Plate flexural rigidity;
x	Longitudinal coordinate;
y	Transversal coordinate;
z	Vertical coordinate;
M_y	Bending moment, y direction;
σ_x	Normal stress, x direction;
σ_y	Normal stress, y direction;
w	Plate deflection;
a	Plate length (parallel to the model centerline);
b	Plate width (orthogonal to the model centerline);
h	Plate thickness;
q	Amplitude of the spatially uniform load.

MODEL BASIN

The Ocean basin has the following characteristics:

- Main dimensions: length of 40 m, width of 30 m and depth of 15 m; the basin has a central pit with additional 10 m in depth and a diameter of 5 m;
- Windows at the basin walls (1.2 m x 2.0 m) at 5 m depth;
- Multi flap wave generator with 75 wet-back hinged flaps, capable of generating the following directional waves: regular waves with periods from 0.5 s to 5.0 s, with a maximum height of 0.52 m; irregular long- and short-crested waves with a peak period of 3.0 s and maximum significant height of 0.3 m;
- Longitudinal and transversal parabolic beaches for waves absorption with lengths of 8.0 m (longitudinal beach) and 5.0 m (transversal beach);
- Measurement instruments: optical system for 6 DOF movement tracking; wave probes; load cells; and accelerometers;
- Movable floors on the basin and on the central pit hole. Operated by electric winches, they can have their depth adjusted from 2.4 m to 14.85 m on the basin; and from 15 m to 24.85 m on the central pit.

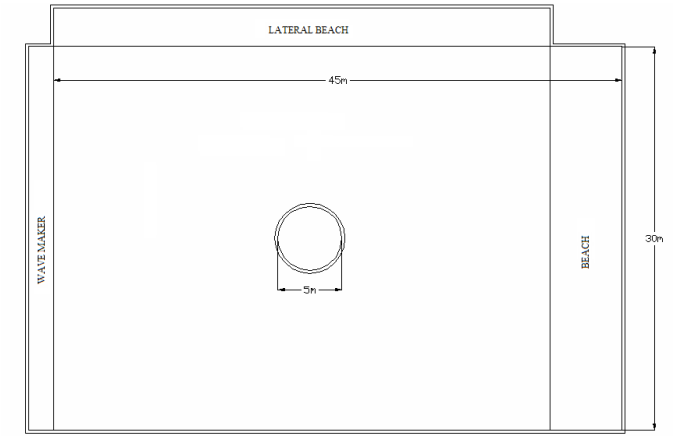

Figure 1: Elevation plan of ocean basin

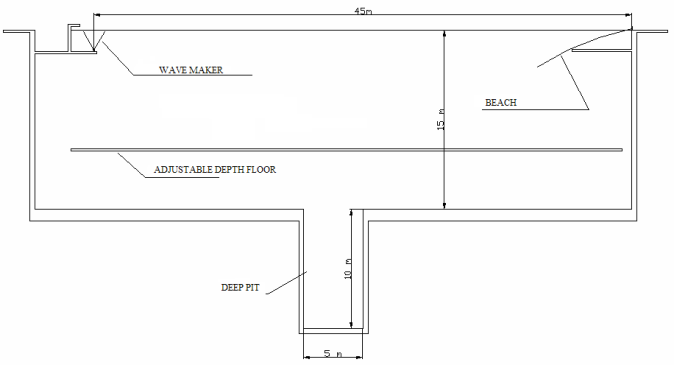

Figure 2: Lateral view of the ocean basin

INSTRUMENTATION AND CALIBRATION

The following instrumentation was used: "Krypton" visual tracking system to measure the 6 DOF motions of the hull; capacitive wave-probes to measure wave heights; load cells for mooring line tensions, and strain gages for measurements of the bilge keels loads. Figures 3 and 4 show the sensor locations on the basin and on the model.

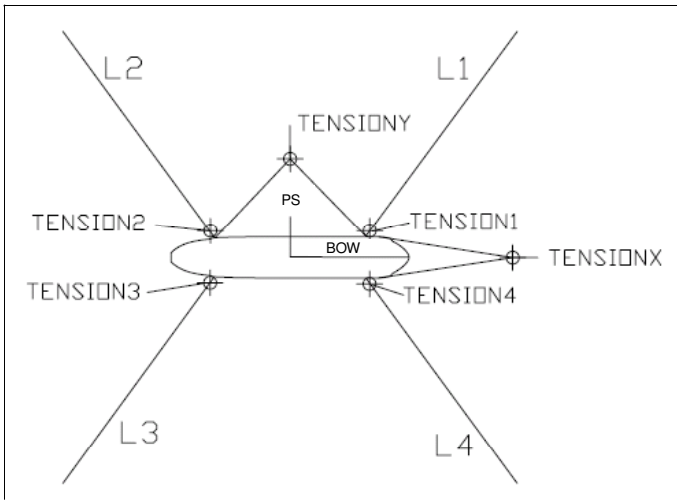

Figure 3: Load cells configuration

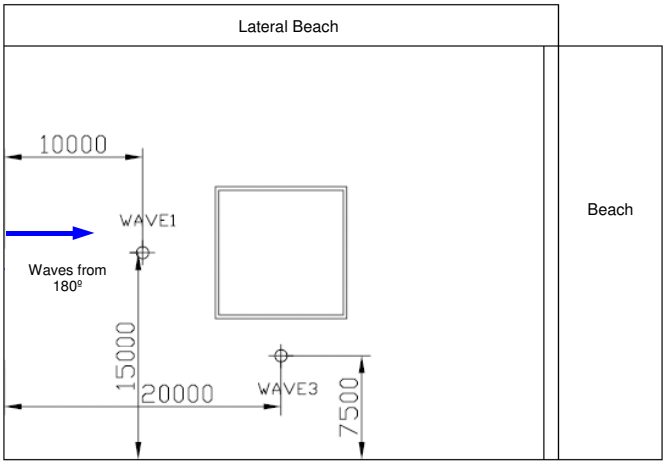

Figure 4: Wave probes location (in millimeters)

MODEL CONSTRUCTION AND CALIBRATION

A model of an FPSO for a deepwater offshore development in Brazil, which included sponsons to make the hull double-sided, was tested. The model was adapted to receive different bilge keels for the model tests. The full-scale main dimensions and characteristics are listed below:

A scale of 1:70 was chosen so that the model would have a sufficient size to minimize scale effects. However, it is important to keep in mind that the flow around the bilge keel may differ from the experiments to the prototype scale due to

the fact that viscous effects scale differently than potential effects, complicating the interpretation of the results.

Table 1: Hull properties (full scale)

Item	Full load	Ballast	Unit
Length bet. perpendiculars	316.0		m
Beam	57.2		m
Depth	28.3		m
Draft	21.7	6.7	m
Displacement	317803	79166	tons
KG	15.4	18.2	m
LCG (from AP)	10.0	13.5	m
GM_T	8.1	29.6	m
Radius of gyration in roll	18.4	21.7	m
Radius of gyration in pitch	76.2	87.6	m
Radius of gyration in yaw	77.9	88.9	m

Figure 5: Finished model, showing the hull sponsons

The hull was made of "Divinycell". First, templates were built based on the shiplines supplied by Shell. A plug was constructed in wood, and its dimensions were verified. Then, a fiberglass mold was extracted from the plug. The final hull was obtained using the mold, by laminating fiber and resin inside of it. An internal structure made of wood was mounted on the fiberglass model. The model parts were then assembled by using a reference frame.

The mass of the light model was measured, followed by estimates of the CG and inertia, obtained by means of moment measurements and free oscillation bifilar tests. Based on the required characteristics and measured light model mass properties, a weight plan was defined to calibrate the model to the correct mass characteristics. The cross-product inertias of the model were considered zero due to the model and ballast symmetries. The tolerances desired for model calibration were 5% for mass and for the inertias that are relevant to the tests, as suggested on specialized literature [1]. The model was eventually placed in the water and the waterline marks were checked. It was verified that the model waterline was within the tolerances defined (±1.5 mm).

MOORING SYSTEM AND ITS CALIBRATION

The model was moored by 4 horizontal lines with springs. The system stiffness in sway was specified as 800 kN/m in prototype scale, to avoid the drifting of the model during the tests. Figure 6 shows the fairlead points on the model, while Figure 7 11 shows the mooring lines positioning on the basin.

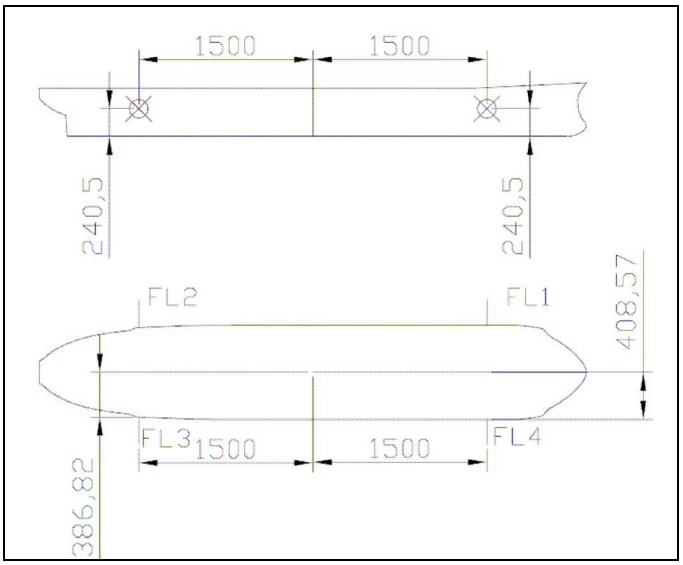

Figure 6: Fairleads positions, model scale

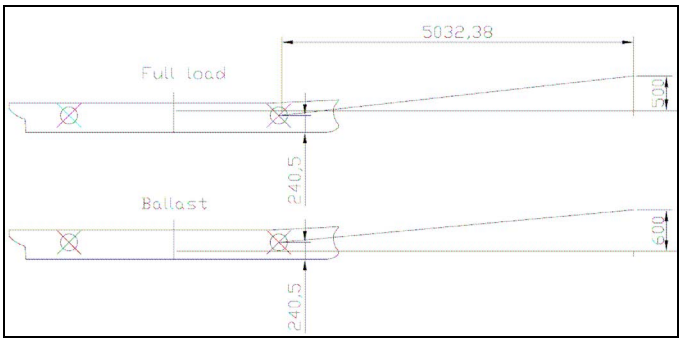

Figure 7: Mooring line configuration

The mooring stiffness in the surge and sway directions were measured in pullout tests. In the prototype scale, the surge stiffness was estimated to be 507.6 kN/m, while the sway stiffness was estimated to be 772.8 kN/m.

BILGE KEEL THEORETICAL MODELLING

In order to measure the wave loads acting on the bilge keels, the following simplifying assumptions were imposed:

i) The fluid loading on the bilge keel is assumed spatially uniform both in x-direction (bow-stern direction) and y-direction (starboard-port direction) of the plate. This assumption of uniformity in the x-direction is reasonable for beam seas conditions, especially at the parallel middle body part of the hull. To improve this assumption, the

length of the bilge keel was divided in five segments. The assumption of spatial uniformity in the y-direction is an approximation, because there is a load variation at least in a narrow region close to the bilge keel free edge.

ii) The lowest natural frequency of the bilge keel considered as a structural element is much higher than the wave frequencies (see for example Table 11-9, pg. 275, [2]). As a result, no dynamical interferences are expected in the measurements. So, it is assumed that the time dependence of the spatially uniform load intensity q does not affect the bilge keel measurements.

iii) The plate is very long (the aspect ratio for the largest bilge keel is higher than 6). So, following the recommendations of [3], the rectangular plate was modeled as a strip (one-dimensional theory).

iv) The strain gage circuit was calibrated using several constant weight loads, in order to obtain the gain factor.

Classical Plate Theory

Figure 8 shows the main dimensions of the bilge keel modeled as a plate.

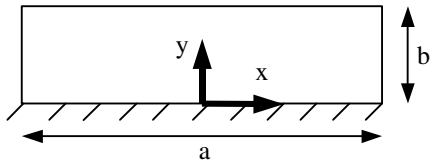

Figure 8: Bilge keel dimensions and reference frame

The main equations of Classical Plate Theory are:

$$M_x = -D\left(\frac{\partial^2 w}{\partial x^2} + \nu\frac{\partial^2 w}{\partial y^2}\right); \quad \text{(Bending moment, x direction; 1)}$$

$$M_y = -D\left(\frac{\partial^2 w}{\partial y^2} + \nu\frac{\partial^2 w}{\partial x^2}\right); \quad \text{(Bending moment, y direction; 2)}$$

$$\frac{\partial^4 w}{\partial x^4} + 2\frac{\partial^4 w}{\partial x^2 \partial y^2} + \frac{\partial^4 w}{\partial y^4} = \frac{q}{D}. \quad \text{(Lateral deflection equation; 3)}$$

The boundary conditions for the bilge keel are:

i) Fixed edge (attached to the hull):

$$(w)_{y=0} = 0; \quad \text{(No deflection; 4)}$$

$$\left(\frac{\partial w}{\partial x}\right)_{y=0} = 0. \quad \text{(No rotation; 5)}$$

ii) Free edge:

$$\left(\frac{\partial^2 w}{\partial x^2} + \nu\frac{\partial^2 w}{\partial y^2}\right)_{y=b} = 0; \quad \text{(No bending moment; 6)}$$

$$\left[\frac{\partial^3 w}{\partial x^3} + (2-\nu)\frac{\partial^3 w}{\partial x \partial y^2}\right]_{y=b} = 0. \quad \text{(Kelvin-Kirchoff condition; 7)}$$

Long Rectangular Plates

After imposing the simplifying assumptions mentioned above, the bending of a long rectangular plate subjected to a uniform transverse load is solved based on the one-dimensional plate theory. The deflected surface of such plate (far from the ends) can be assumed cylindrical and the strain will occur only in the y-direction (ε_y). So, the following equations are derived:

$$\varepsilon_x = \frac{\sigma_x}{E} - \frac{\nu\sigma_y}{E} = 0; \quad (8)$$

$$\sigma_y = \frac{E\varepsilon_y}{1-\nu^2} = -\frac{Ez}{1-\nu^2}\frac{d^2 w}{dy^2}; \quad (9)$$

$$M_y = \int_{-h/2}^{h/2} \sigma_y z\,dz = \frac{Eh^3}{12(1-\nu^2)} w''; \quad (10)$$

$$D = \frac{Eh^3}{12(1-\nu^2)}; \quad (11)$$

$$D\frac{d^2 w}{dy^2} = -M_y; \quad \text{(Equation of the deflection curve; 12)}$$

$$\varepsilon_y = -zw''; \quad \text{(Strain equation; 13)}$$

$$\varepsilon_y = -\frac{h}{2}w''. \quad \text{(Upper surface strain, at z = h/2; 14)}$$

Consider now a strip of a long rectangular plate with one edge fixed (attached to the hull) and the opposite edge free, as shown in Figure 9. The load is uniformly distributed with intensity q.

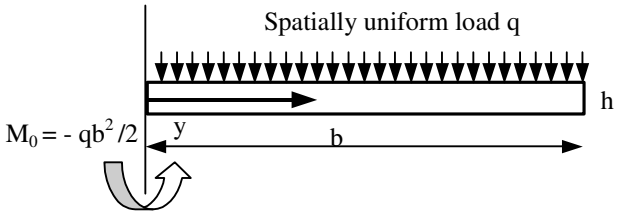

Figure 9: Bilge keel (long rectangular plate)

The bending moment for this uniform load is

$$M_y = qby - q\frac{y^2}{2} - q\frac{b^2}{2}. \quad (15)$$

The deflection equation is given by:

$$D\frac{d^2 w}{dy^2} = -M_y. \quad (16)$$

So, the differential equation for the strip (long plate) is similar to beam theory (with D taking the place of EI). The deflection curve is given by the following equation:

$$w(y) = -\frac{qb}{2D}\frac{y^3}{3} + \frac{q}{6D}\frac{y^4}{4} + \frac{qb^2}{2D}\frac{y^2}{2}. \quad (17)$$

The maximum deflection is obtained at the position y=b (free edge):

$$w_{max} = w(b) = 0.125\frac{qb^4}{D}. \quad (18)$$

This result (long plate, strip theory) is identical to the complete analytical solution [3-5]. So, it is confirmed that for a long plate (b/a < 1/3) under the action of a uniform load, the two-dimensional plate theory can be replaced by the one-dimensional theory (strip theory) without a substantial error (page 120, [3]).

The strain can now be evaluated by using the equation:

$$\varepsilon_y = -zw''. \quad (19)$$

The strain at the upper surface (z = h/2) is given by:

$$\varepsilon_y = -\frac{h}{2}w'' = -\frac{hq}{2}\left(-\frac{b}{D}y + \frac{1}{2D}y^2 + \frac{b^2}{2D}\right) \quad (20)$$

So, for a long plate (with one fixed and three free edges) the strain at the upper surface is a quadratic function of y. The maximum strain occurs at the fixed edge (y = 0, at the hull surface). It can be observed as well that for a uniformly distributed load, there is a linear relationship between the strain (at a fixed y coordinate) and the load intensity q [6,7].

For example, fixing the strain gage circuit at the mean position (y = b/2), one has:

$$\varepsilon_y\Big|_{y=b/2} = -\frac{h}{2}w'' = -\frac{h}{2}\left(-\frac{qb}{D}\frac{b}{2} + \frac{q}{2D}\left(\frac{b}{2}\right)^2 + \frac{qb^2}{2D}\right) = -\frac{hqb^2}{16D}. \quad (21)$$

The strain (and the electrical signal) can be amplified by reducing the plate thickness (h) [8-10]. But one has to be cautious in order to avoid very large strains. Another way to amplify the signal is by positioning the strain gage circuit closer to the fixed edge (y = 0).

MEASUREMENT OF BILGE KEELS FORCES AND CALIBRATION

For the measurement of the model's bilge keels forces, 2 mm strain gages were used. The bilge keels were made of metal, so that an array of strain gages could be mounted on them. Ten strain gages were placed in the middle of each of the bilge keel instrumented segments, which scaled to a length of 21 m and were located along the parallel middle body of the hull. For each of the two bilge keels, the total length was about 200 m, while the total instrumented length was 105 m.

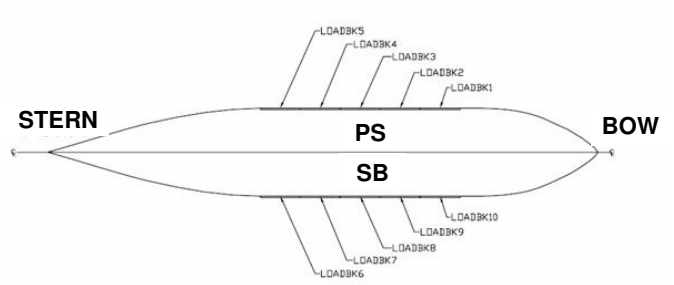

Figure 10: Bilge keel forces gauges configuration

The bilge keels were designed to be interchangeable, so that bilge keels with different widths (1, 2 and 3 m) could be quickly removed and/or attached to the model. To accomplish that, beams with an "L"-shaped cross-section were used as bilge keels, with one flat surface connected to the model bilge by means of screws, and the other modeling the bilge keel itself.

The bilge keel strain-gage circuit calibration (to obtain gain factors) was performed by applying known uniform loads on the bilge keel segments and measuring the strain-gage response (voltage). In general, for the range tested, the voltage is linearly correlated to the loads, as anticipated theoretically.

However, for some bilge keel segments, the linear gain factor measured for deflections in one direction was different than that measured for deflections in the opposite direction. This was attributed to asymmetries in the geometry of the bilge keel segments, which were manually bent and drilled to accommodate the screws. Thus, gain factors that were different for each direction of deflection were used to obtain the bilge keel loads. To minimize the difference between the measurements of the different bilge keel segments, the average of the loads was used in the analyses.

GENERATION OF WAVES AND CALIBRATION

The waves were first calibrated without the model in the basin, so that incident waves could be measured. To accomplish that, a setup with 3 wave probes was used.

The wave probe called WAVE2_C was used to measure the incident wave since it was installed on the further model position. WAVE1_C and WAVE3_C were used for synchronism and checking.

a) Regular Waves: Each wave was calibrated to have its period and height within defined tolerances (±3%). The calibration was done first by measuring the waves, and then implementing a gain on the wave maker to adjust eventual discrepancies to the required values.
b) Random Waves: Tolerances for random waves are also 3% from the required values (for the significant height and

peak period). The maxima and minima points are also analyzed to avoid non-Gaussian events. If this occurs, the wave is run again with a different seed number for the random phases generation.

c) Bimodal Seas: For the generation of bimodal seas (representing a sea and swell condition), at first each component was calibrated separately, and then the calibrated components were generated together on the basin.

MODEL TESTS RESULTS

The test program was divided in groups, each group having a different combination of load condition (or draft), wave heading and bilge keel width. Even though two draft conditions were tested, this paper only presents results for the loaded condition.

DECAY TESTS

Roll decay tests were performed using thin cables and pulleys to heel the model without changing the mean draft. This was an attempt to apply a pure moment (or as close as possible) to the model. After the model stabilized in the desired angle, the cable was cut, and the model was free to oscillate. The decay tests for the other DOFs were done by using single cables with a procedure similar to the roll tests.

The decay tests are analyzed for the system described as freely oscillation according to the expression below:

$$\ddot{\phi} + p_1\dot{\phi} + p_2\left|\dot{\phi}\right|\dot{\phi} + p_3\dot{\phi}^3 = 0\,, \tag{22}$$

where: ϕ – motion of interest;
p1 – linear damping coefficient;
p2 – quadratic damping coefficient;
p3 – cubic spring coefficient.

The energy method for evaluating the damping coefficients calculates the energy dissipated by the system in one half cycle, by integrating Eq. 22:

$$\delta\phi_{i+1} = \frac{\pi p_1}{2\omega}\phi_m + \frac{4p_2}{3}\phi_m^2 + \frac{3\pi p_3\omega}{8}\phi_m^3\,. \tag{23}$$

If one takes the first two parameters of Eq. 22, and considers a linear coefficient "pe" with the same energy as Eq. 23, the following expression results:

$$pe = \frac{2}{T_m}\log\left(\frac{X_{n-1}}{X_{n+1}}\right) = p_1 + \frac{16X_n}{3T_m}p_2\,, \tag{24}$$

where X_n is the n^{th} amplitude and T_m the oscillation period.

For a given decay test, the values of $2/T_m \log(X_{n-1}/X_{n+1})$ can be plotted against the term $16X_n/3T_m$, so that coefficients p_1 and p_2 can be obtained by using linear regression. This approach is known as linear approximation.

Other damping coefficients can also be obtained by plotting and then adjusting a quadratic or even a cubic curve for $f(\phi_m)$. Another possible regression of decay tests is a linear adjustment of the decrease of the motion amplitude, divided by the mean motion amplitude, given as a function of the mean motion amplitude, known as equivalent damping. For this approach, p and q coefficients (calculated values are shown in Tables 2 and 3 for different loading conditions) are given by:

$$\frac{(\phi_{n+1} - \phi_n)}{\frac{1}{2}(\phi_{n+1} + \phi_n)} = p + q\left(\frac{1}{2}(\phi_{n+1} + \phi_n)\right). \tag{25}$$

Table 2: Decay tests average results for the loaded condition

Bilge Keel Width (m)	Roll T_n (s)	p	q
0	13.61	0.0692	0.0045
1	13.76	0.1142	0.0167
2	13.98	0.1098	0.0402
3	14.08	0.1339	0.0562

Table 3:Decay tests average results for the ballast condition

Bilge Keel Width (m)	Roll T_n (s)	p	Q
0	9.867	0.3111	0.0044
1	10.038	0.3021	0.0488
2	10.349	0.3047	0.0770
3	10.701	0.3247	0.0857

ROLL

Regular Waves Tests

Figure 11 shows a sample of the roll motions measured for different bilge keels widths in regular waves. One can clearly see the influence of the bilge keel size on the roll damping.

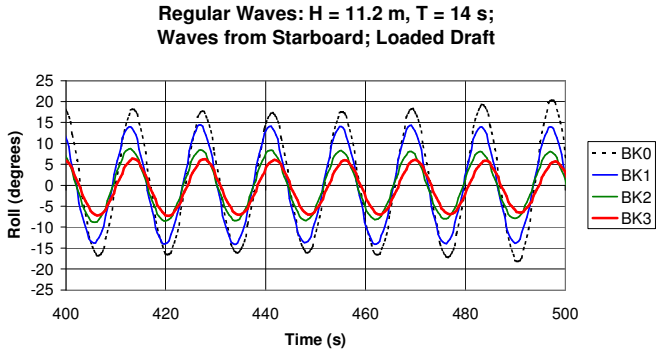

Figure 11: Roll motion for different bilge keel widths in regular waves

Random Waves Tests

Figure 12 shows a sample of the roll motions for different bilge keels widths in irregular waves (JONSWAP spectrum).

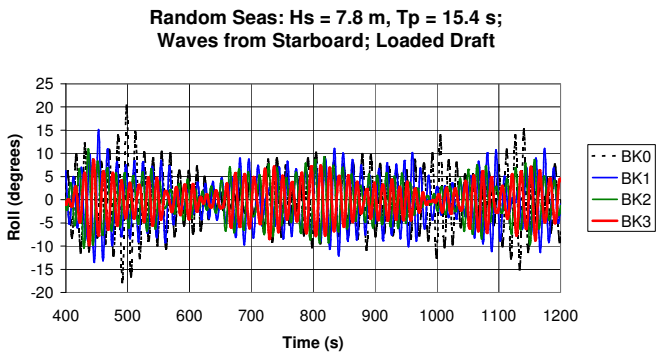

Figure 12: Roll motion for different bilge keels widths in random seas

Figure 13 shows the Roll RAO for beam seas derived from four different seastates. All the values shown are for bilge keel width of 1 m and beam seas. Due to the quadratic term in roll damping, the RAO values are higher for the lower seastates.

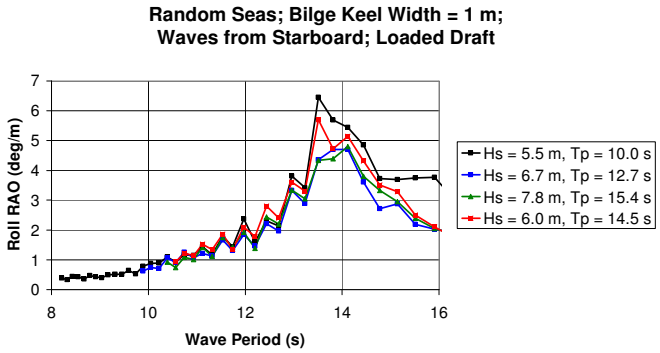

Figure 13: Roll RAO derived from four random seastates

Figure 14 shows the Roll RAO values for beam seas derived for the four different cases of bilge keels. All the values shown are for the lowest significant wave height seastate and beam seas. Due to the quadratic term in roll damping, the RAO values are higher for the lower seastates.

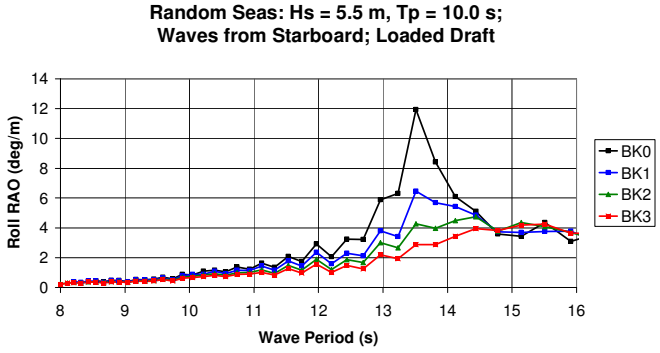

Figure 14: Roll RAO for different bilge keels

Figure 15 shows measured roll motion maxima and minima (black lines) and standard deviation around the mean value (shaded bars) for irregular beam seas. We can see, as expected, the progressive reduction of the roll motion amplitudes due to the enlargement of the bilge keel width and roll damping. However, the dependence with the wave periods is also noted: for Hs = 6.0 m and Tp = 14.5 s, close to the natural roll period for this configuration, the roll response is larger than that observed for Hs = 6.7 m and Tp = 12.7 s.

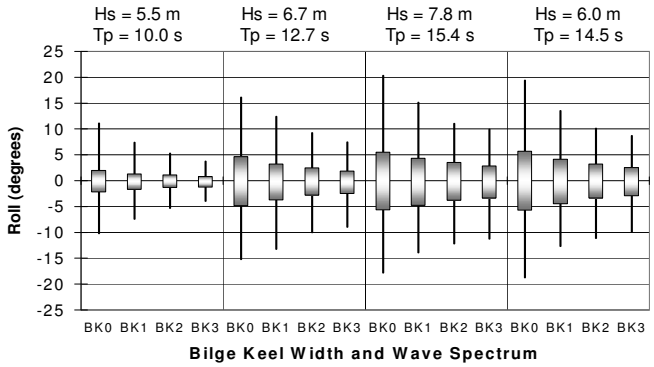

Figure 15: Roll motion vs. bilge keel width and wave spectrum (waves from starboard, loaded draft)

Figure 16 shows the same quantities as Figure 15 for Hs = 7.8 m and Tp = 15.4 s, but for different wave incidence angles. Again, we can verify a large reduction of the roll motion according to the incidence angle reduction.

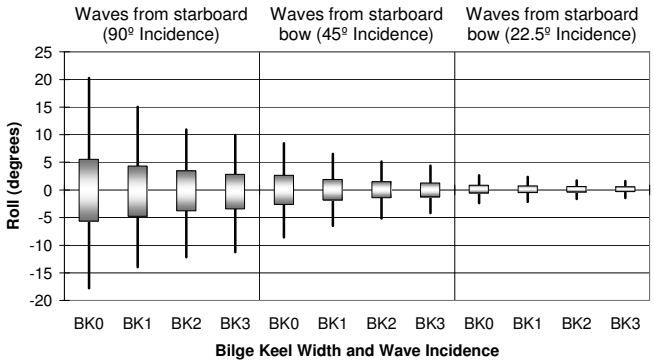

Figure 16: Roll motion vs. bilge keel width and wave incidence angle (Hs = 7.8 m, Tp = 15.4 s; loaded draft)

BILGE KEEL LOADS

Figure 17 shows the average of the measured loads for all bilge keels segments on both sides of the hull (PS = port side; DW = down waves; SB = starboard; UW = up waves), for a regular waves test. Figures 18, 19, 20, and 21 show the average of the bilge keel segments loads for two irregular beam seas. The large difference between the starboard and port side values of the loads could at first be attributed to the more intense wave

action at the starboard side of the FPSO, in comparison to the port side (shadow region). In regular beam seas the formation of stationary waves at the starboard side of the FPSO due to wave reflections was clearly observed during the experiments.

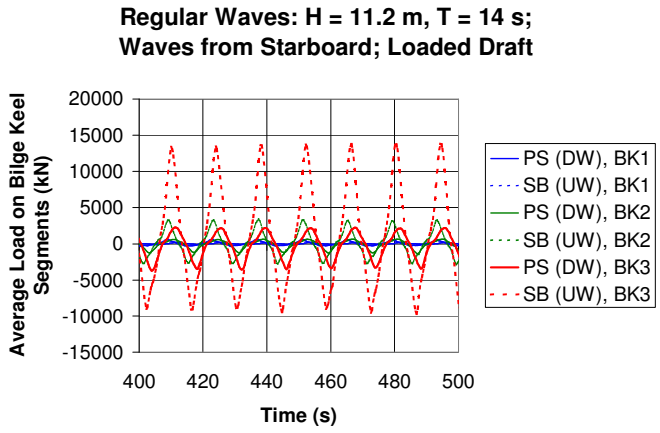

Figure 17: Average bilge keel loads for different bilge keel widths in regular waves

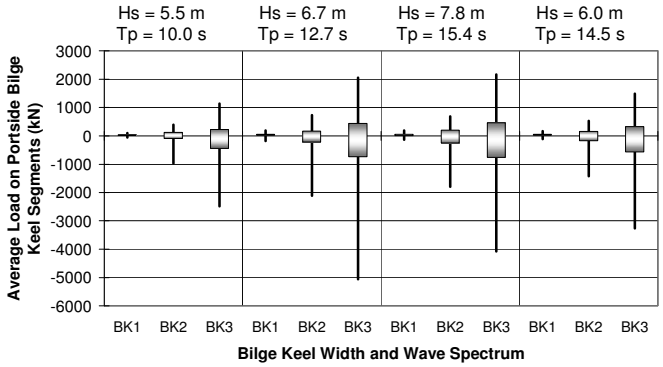

Figure 18: Down waves bilge keel load vs. bilge keel width and wave spectrum (waves from starboard, loaded draft)

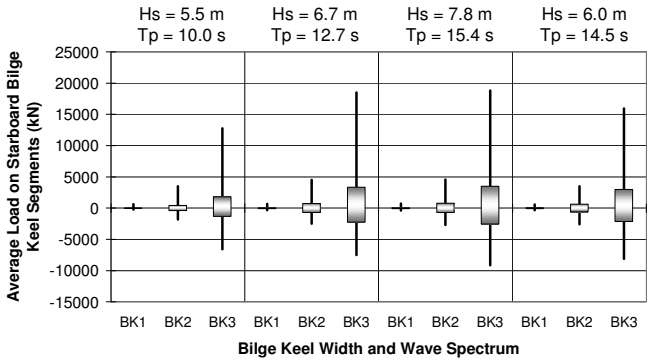

Figure 19: Up waves bilge keel load vs. bilge keel width and wave spectrum (waves from starboard; loaded draft)

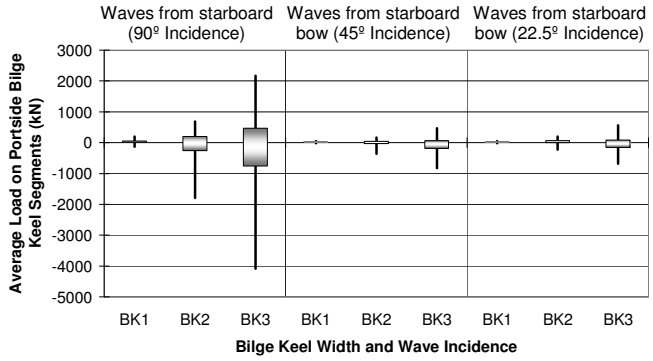

Figure 20: Down waves bilge keel load vs. bilge keel width and wave incidence angle (Hs = 7.8 m, Tp = 15.4 s; loaded draft)

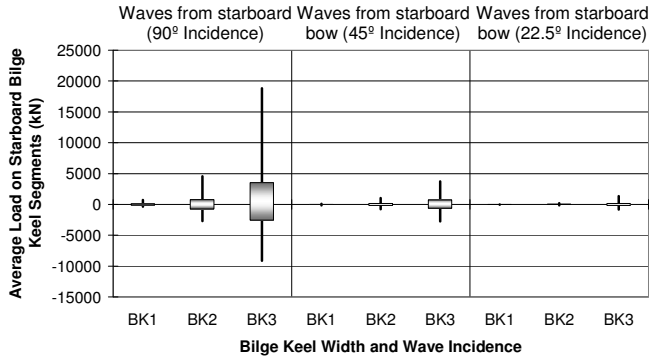

Figure 21: Up waves bilge keel load vs. bilge keel width and wave incidence angle (Hs = 7.8 m, Tp = 15.4 s; loaded draft)

CONCLUSIONS

Model tests of an FPSO with and without bilge keels in waves were undertaken. The influence of bilge keels of three different widths on the motions was assessed. A new method of measuring the forces on the bilge keels was developed, consisting of employing strain gages to measure the deflections of the bilge keels, and using plate theory to compute the force from the bilge keel strains. The motions of the FPSO were measured in regular and random waves. As expected, the roll motions decrease with an increase in the width of the bilge keels. The load on the bilge keels also increases with width. In addition, due to the higher relative motions and the disturbances in the wave field, the bilge keel loads on the incident waves side of the model are much higher than the loads on the opposite side.

ACKNOWLEDGMENTS

This effort was funded by the Shell Brazil E&P Bijupirá-Salema Research and Development Obligation.

REFERENCES

[1] Chakrabarti, S. K., 1994, Offshore Structures Modeling, Advanced Series on Ocean Engineering – Volume 9, World Scientific.

[2] Blevins, R.D., 1979, Formulas for Natural Frequency and Mode Shape, Van Nostrand Reinhold.

[3] Timoshenko, S.P. and Woinowsky-Krieger, S., 1959, Theory of Plates and Shells, 2nd Edition, International Student Edition, McGraw-Hill.

[4] Shames, I.H. and Dym, C.L., 1985, Energy and Finite Element Methods in Structural Mechanics, McGraw-Hill.

[5] Hughes, O.F., 1983, Ship Structural Design: A Rationally-Based, Computer-Aided, Optimization Approach, Wiley Series on Ocean Engineering, John Wiley & Sons.

[6] Kara, F. and Vassalos, D., 2006, "Hydroelastic analysis of cantilever plate in time domain", Ocean Engineering, **34**, 1, p. 122-132.

[7] Rossi, R.E., Belles, P.M., Laura, P.A.A., La Malfa, S., Ercoli, L., and Pasqua, D., 1996, "Transverse vibrations of a rectangular cantilever plate with thickness varying in a discontinuous fashion", Ocean Engineering, **23**, 3, p. 271-276.

[8] Doebelin, E.O., 1990, Measurements Systems: Application and Design, McGraw-Hill.

[9] Holman, J.P., 1989, Experimental Methods for Engineers, 5th Edition, Engineering Series, McGraw-Hill.

[10] Figlioga, R.S. and Beasley, D. E., 1995, Theory and Design for Mechanical Measurements, 2nd Edition, John Wiley & Sons.